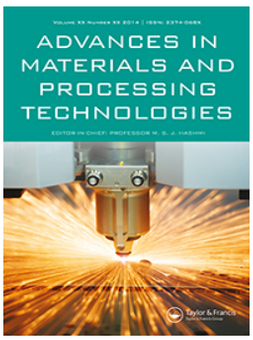

Advances in Materials and Processing Technologies

ISSN: (Print) (Online) Journal homepage: https://www.tandfonline.com/loi/tmpt20

# Modelling of material removal rate and tool wear rate in EDM based on a fraction of energy approach

C. R. Sanghani , G. D. Acharya & K. D. Kothari

**To cite this article:** C. R. Sanghani , G. D. Acharya & K. D. Kothari (2020): Modelling of material removal rate and tool wear rate in EDM based on a fraction of energy approach, Advances in Materials and Processing Technologies, DOI: 10.1080/2374068X.2020.1796165

**To link to this article:** https://doi.org/10.1080/2374068X.2020.1796165

Published online: 05 Aug 2020.

Submit your article to this journal

Article views: 2

View related articles

View Crossmark data

Full Terms & Conditions of access and use can be found at
https://www.tandfonline.com/action/journalInformation?journalCode=tmpt20

ADVANCES IN MATERIALS AND PROCESSING TECHNOLOGIES
https://doi.org/10.1080/2374068X.2020.1796165

Taylor & Francis
Taylor & Francis Group

Check for updates

# Modelling of material removal rate and tool wear rate in EDM based on a fraction of energy approach

C. R. Sanghani[a], G. D. Acharya[b] and K. D. Kothari[c]

[a]School of Engineering, R.K. University, Rajkot, India; [b]Atmiya Institute of Technology and Science, Rajkot, India; [c]Mechanical Engineering Department, School of Engineering, R. K. University, Rajkot, India

**ABSTRACT**

To run any machine effectively and economically, the effect of different process variables on the performance must be known. An experimental investigation is costly, time-consuming as well as difficult for a complete understanding of the EDM process. Hence, several researchers have developed various models of the process using different approaches like mathematical modeling, finite element analysis, regression modeling, dimensional analysis, etc. based on certain assumptions and simplifications, which limit the accuracy of prediction. In this article, a novel modeling approach is presented to predict material removal rate (MRR) and tool wear rate (TWR) during machining of AISI D2 tool steel by the copper electrode using the full factorial design. The validation was carried out using Taguchi's L9 orthogonal array-based confirmation experiments. The results showed that these models can be used for prediction of MRR and TWR at any set of process parameters for a given combination of workpiece and tool with good accuracy.

**ARTICLE HISTORY**
Accepted 13 July 2020

**KEYWORDS**
EDM; MRR; TWR; Modeling; regression

## 1. Introduction

For the material removal mechanism in the electrical discharge machining process, different theories like electro-mechanical, thermo-mechanical, and thermo-electric have been proposed. But, Lazarenko's thermo-electric theory is the most popular for an explanation of the material removal process in EDM. According to this theory, the material gets removed due to the generation of extremely high temperature between workpiece and tool in the presence of a dielectric medium. It is difficult to represent the EDM process by a simple model due to the involvement of several subjects like thermodynamics, hydrodynamics, electrodynamics, and electromagnetism [1]. Different modeling approaches have been attempted by researchers to predict the performance of the EDM process. Dibitonto et al. [2] developed a cathode erosion model for EDM considering point heat source and a constant fraction (Fc = 0.183) of the total power transfer to the cathode using the photoelectric effect as the dominant source of energy while the anode erosion model was presented by Patel et al. [3] with the assumption of time-varying Gaussian-distributed heat flux on the anode surface. Based on a variable mass, cylindrical plasma model (VMCPM), Eubank et al. [4] showed that the superheating is the

**CONTACT** C. R. Sanghani scr1385@yahoo.com School of Engineering, R.K. University, Rajkot, Gujarat 360020, India

© 2020 Informa UK Limited, trading as Taylor & Francis Group

dominant mechanism for erosion in EDM. Gulbinowicz et al. [5] developed a mathematical model of material erosion during single electrical discharge machining of structural steel C45 and tungsten heavy alloys (WSC). It was found that current density and pulse on time have a dominant effect on crater volume. Singh and Ghosh [6] calculated crater depth using a thermo-electric model by estimating the electrostatic force responsible for material removal in short pulses (<5 μs). To estimate the geometrical dimensions of micro-crater, Yeo et al. [7] proposed analytical models of anode and cathode using electro-thermal theory. Salonitis et al. [8] also developed thermal-based analytical models of the MRR and the average surface roughness as a function of the process parameters. Using dimensional analysis, Wang and Tsai [9] established a semi-empirical model for MRR as well as TWR, and results showed that this model cannot be represented by a set of universal coefficients and power indexes due to their dependency on the materials. Several other researchers (Jeswani [10], Tsai and Wang [11], Dave et al. [12], Kumar et al. [13], Yahya and Manning [14], Bhaumik et al. [15]) also used dimensional analysis approach for modeling of MRR, TWR, surface roughness, overcut, etc. at different conditions of machining. Schulze et al. [16] investigated the crater morphology of EDM by comparing the measured and simulated crater for single discharge and a sequence of discharges using combined results of confocal laser scanning microscopy (CLSM), high-speed framing camera (HSFC) and ANSYS. Lasagni et al. [17] carried out a thermal analysis of EDM by FEA in FlexPDE software using a point heat source and found that the melting enthalpy and the melting point can control the material removal. For the prediction of crater shape and MRR, Joshi and Pande [18] developed a two-dimensional axisymmetric model of single spark based on realistic assumptions like variable spark radius, Gaussian heat distribution, latent heat of melting, etc. A hybrid model for EDM, based on the finite-element method (FEM) and Gaussian process regression (GPR) was proposed by Ming et al. [19] for prediction of MRR and surface roughness by considering the latent heat, variable heat distribution factor of the cathode and plasma flushing efficiency. Tang and Yang [20] proposed the thermo-hydraulic coupling model of discharge crater formation using COMSOL software to understand the material removal process in EDM. Zhang et al. [21] derived a spark column expansion formula based on the time integration effect (TIE) and developed a finite element thermal model considering that effect to predict the craters and MRR. A theoretical thermal model and 3D finite element model were developed by Yildiz [22] for the prediction of material removal rate and white layer thickness. The average prediction errors for MRR and white layer thickness were found 3.34% and 1.98% respectively. An iterative-based statistical approach has been presented by Assarzadeh and Ghoreishi [23] for prediction of root mean square roughness parameter (Rq) for EDMed surface considering successive discharges and plasma flushing efficiency (PFE). It is also found that the predictive accuracy of the model can be improved by considering plasma flushing efficiency. A new approach based on the specific discharge energy (SDE) was proposed by Huang et al. [24] to predict the performance of different materials under various machining conditions. They computed the value of SDE from a numerical model of the EDM process developed considering the different proportions of the energy distribution and equivalent temperature. Wu et al. [25] investigated the effects of discharge energy level on crater size, phase transformation, and residual stress during EDM of Ti-6Al-4 V alloy using the FEM model based on ABAQUS. The phase transformations during EDM were modeled based on kinetics and flow stress. Klocke et al. [26] investigated the variation in existing simulation models for single discharge in EDM and concluded that the use of heat distribution factor and heat source model without considering the difference in

governing conditions leads to inaccurate results. The solution for this problem could be the reverse simulation in which the unknown parameters (heat distribution factor, plasma channel radius) in EDM simulation would be changed to match the experimental results. Jatti and Bagane [27] used ANSYS software to simulate powder mixed EDM of Beryllium copper alloy and to predict MRR. The average error of prediction was found 7.8%. Jithin et al. [28] proposed a finite element model for a single spark in EDM considering realistic assumptions. The results showed that crater radius and depth increases with an increase in discharge current and pulse on time due to an increase in input energy and the duration of heat flux. The prediction error of the FE model for the crater aspect ratio (radius/depth) was found from 9.1 to 13.4%. Bergs et al. [29] used a combined approach of heat transfer and fluid dynamics. The results showed that convective cooling has a negligible effect on the workpiece surface during a single discharge but it may have a significant effect during continuous sparking. A micro-EDM of bulk metallic glass (BMG) was investigated by Liu et al. [30] and they found that micro-EDM can generate crater as small as 2.2 μm. The simulation of a single crater during micro-EDM of BMG was carried out using ABAQUS software and it showed that each crater is associated with a molten phase, crystalline phase, and supercooled liquid phase. This model can be used to predict the crystallization and recast layer thickness. Puertaset et al. [31] used a response surface methodology to develop multiple regression equations for material removal rate, electrode wear, and surface roughness. The empirical models were developed by Chattopadhyay et al. [32] for the prediction of output parameters using non-linear regression with logarithmic data transformation. A regression model was proposed by Izwan et al. [33] to predict the MRR for four different materials Aluminum 6061-T6, Domex 550MC steel, HSLA steel, Brass CA 360 and compared with a published model. The result showed that the prediction error for the proposed model is about two orders of magnitude lower as compared to that from a published model. Puthumana [34] developed a model for TWR in micro-EDM of biocompatible microdevices using multiple linear regression analysis (MLRA). The model was found to be significant at a 90% confidence level and hence and could be used for prediction where high precision is not required. Hosni et al. [35] used RSM to develop a model of recast layer in powder mixed EDM of AISI D2 steel and desirability function to find optimum parameters for the minimum recast layer. A blind hole of 30 micron depth in Ti-alloy was analyzed by Perveen and Jahan [36] to predict the values of crater size. It was concluded that response surface methodology with Box-Behnken design could be used to develop a model for prediction of crater size created during micro EDM with a medium level of the discharge energy. The models developed by dimensional analysis have a limitation of material dependency and hence the values of coefficients as well as power indexes can't be used universally. The mathematical models are developed under several assumptions for the simplicity of models and hence they have limited prediction accuracy. In numerical modeling technique, more real-time conditions like flushing efficiency, recast layer, a variable fraction of energy transfer to workpiece and tool, multiple discharges, etc. are required to increase prediction accuracy. The models developed by statistical technique have not good prediction accuracy for the process parameters which are out of the considered range for developing the models. So, a novel approach for modeling based on the combination of fundamental theory and regression method is developed and discussed here.

Table 1. Process parameters and their levels.

| | | | Levels | | |
|---|---|---|---|---|---|
| Factors | Parameters | Symbol | Low (1) | Medium (2) | High (3) |
| A | Discharge current (A) | I | 6 | 9 | 15 |
| B | Pulse on time (μs) | $T_{on}$ | 100 | 200 | 500 |
| C | Pulse off time (μs) | $T_{off}$ | 20 | 50 | 100 |

## 2. Experimental procedure

### 2.1. Process parameters and performance measures

Three process parameters, viz., discharge current, pulse on time, and pulse off time were identified and their levels were fixed as shown in Table 1. During experimentation, the room temperature was 34° C and the voltage was kept constant at 18 V. The responses studied were MRR and TWR.

### 2.2. Design of experiments

In the development of mathematical models, all combinations of input parameters must be considered to include the influence of input parameters on output responses in different combinations. Hence, a three-factor three-level full factorial design for the present work was used as shown in Table 2.

Table 2. Factorial design matrix ($3^3$ levels) for experimentation.

| | Machine setting | | |
|---|---|---|---|
| Experiment No. | Discharge current | Pulse on time | Pulse off time |
| 1 | 2 | 3 | 3 |
| 2 | 3 | 1 | 3 |
| 3 | 1 | 3 | 3 |
| 4 | 2 | 3 | 2 |
| 5 | 1 | 3 | 1 |
| 6 | 1 | 2 | 1 |
| 7 | 2 | 2 | 2 |
| 8 | 2 | 1 | 1 |
| 9 | 1 | 1 | 3 |
| 10 | 3 | 1 | 1 |
| 11 | 2 | 2 | 1 |
| 12 | 3 | 3 | 2 |
| 13 | 1 | 1 | 2 |
| 14 | 1 | 1 | 1 |
| 15 | 3 | 2 | 2 |
| 16 | 2 | 1 | 2 |
| 17 | 1 | 2 | 3 |
| 18 | 3 | 1 | 2 |
| 19 | 2 | 3 | 1 |
| 20 | 1 | 2 | 2 |
| 21 | 3 | 3 | 3 |
| 22 | 1 | 3 | 2 |
| 23 | 2 | 1 | 3 |
| 24 | 3 | 2 | 1 |
| 25 | 3 | 2 | 3 |
| 26 | 2 | 2 | 3 |
| 27 | 3 | 3 | 1 |

### 2.3. Experimentation

A TOOL CRAFT G30(i) die-sinking EDM machine shown in Figure 1 was used for machining of AISI D2 tool steel by the copper electrode of diameter 12 mm with the positive polarity of the workpiece and negative polarity of the tool. A set of electrodes prepared for working as a tool is depicted in Figure 2. Commercial grade EDM oil with specific gravity 0.77 gm/ltr and flash point 108 °C was used as the dielectric fluid. Table 3 shows the thermophysical properties of the workpiece and tool materials. Each

Figure 1. Spark EDM machine.


**Figure 2.** Set of copper electrodes.

**Table 3.** Thermo-physical properties of workpiece and tool material.

| Property | AISI D2 Tool Steel | Copper |
|---|---|---|
| Density (kg/m$^3$) | 7700 | 8960 |
| Young's modulus (GN/m$^2$) | 208 | 128 |
| Poisson's ratio | 0.3 | 0.34 |
| Thermal conductivity (W/m K) | 29 | 401 |
| Specific heat (J/kg K) | 412 | 385 |
| Melting temperature (K) | 1984 | 1356 |
| Boiling temperature (K) | 2773 | 2840 |
| Latent heat of melting (kJ/kg) | 2746 | 4796 |
| Latent heat of vaporization (kJ/kg) | 1586 | 8960 |

experiment was carried out for 15 minutes. The impressions observed on the work surface by the tool electrode for each experiment are shown in Figure 3.

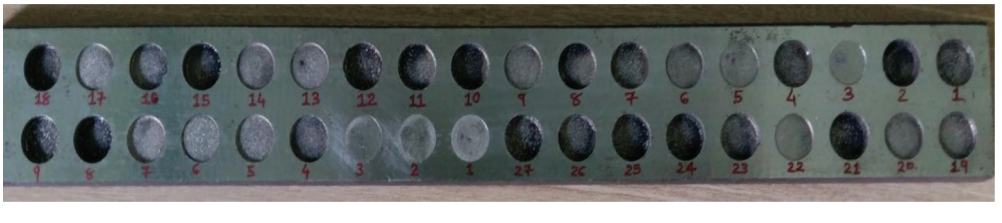


**Figure 3.** Impressions of the tool on work surface after machining.

### 2.4. Measurement of MRR & TWR

The material removal rate (MRR) and tool wear rate (TWR) is the volume of material removed from the workpiece and tool respectively per unit time in $mm^3$/min. For EDM, MRR should be as high as possible and TWR as low as possible to increase productivity. In this work, the TWR was measured by noting the initial and final weights of the tool as well as machining time. The weights of the tool electrode were measured using the Shimadzu AUW220D weighing balance having the least count of 0.0001 g. To calculate MRR, the diameter and depth of tool impressions on the work surface were measured by portable articulated arm coordinate measuring machine (6-axes space 2.5 plus arm) having a range of 2500 mm and point repeatability 0.016 mm. Following equations are used to calculate the material removal rate and tool wear rate:

$$MRR = \frac{\frac{\pi}{4}D^2H}{t_{mach}} \tag{1}$$

$$TWR = \frac{W_1 - W_2}{\rho \times t_{mach}} \tag{2}$$

Where, D = Impression diameter (mm), H = Impression depth (mm) $W_1$ = Initial mass (g), $W_2$ = Final mass (g), ρ = density ($g/mm^3$) and $t_{mach}$ = machining time (min)

## 3. A novel Modeling approach

In EDM, plasma heating causes the melting and vaporization of material from workpiece and tool which generates a crater cavity on the surface. A fraction of energy transfer to workpiece and tool from total discharge energy varies with selected process parameters and it plays a crucial role in material removal from workpiece and tool. Researchers have assumed or selected a fixed value of the fraction of energy transfer in their models and hence over-estimated the value of MRR and TWR. In present work, to have better prediction accuracy, mathematical models for MRR and TWR are developed by varying the value of this factor according to process parameters. The experimental results of MRR and TWR are used to calculate volumetric material removal from the workpiece and tool respectively. The volumetric material removal from workpiece and tool are used to find a fraction of energy transfer to workpiece and tool during the EDM process respectively. The regression equations of the fraction of energy transfer to workpiece and tool are developed which are used to develop models for MRR and TWR.

### 3.1. Material removal rate

The energy responsible for material removal from workpiece [37] is

$$E_{MRR} = \rho V_W \left[C_p(T_v - T_o) + L_m + L_v\right] \tag{3}$$

where ρ – Density ($kg/m^3$), $V_W$ – Volumetric material removal rate from a workpiece ($m^3/s$), $C_p$ – Specific heat (J/kg K), $T_v$–Vaporization temperature (K), $T_o$ – Room temperature (K), $L_m$ – Latent heat of melting (J/kg), $L_v$ – Latent heat of vaporization (J/kg)

The energy released during a single discharge per unit time [38] is

$$E = VI\left(\frac{T_{on}}{T_{on} + T_{off}}\right) \tag{4}$$

where V – Voltage (V), I – Discharge current (A), $T_{on}$ – Pulse on time (μs), $T_{off}$ – Pulse off time (μs)

The fraction of energy (%) responsible for material removal

$$F_{MRR} = \frac{E_{MRR}}{E} \times 100 \tag{5}$$

The regression equation for fraction of energy (%) responsible for material removal derived using statistical software MINITAB 16 is

$$F_{MRR} = 5.2328 \times I^{0.7615} \times {T_{on}}^{-0.2863} \tag{6}$$

Energy responsible for material removal from the workpiece

$$E_{MRR} = F_{MRR} \times E$$

$$= 0.0523 \times I^{0.7615} \times {T_{on}}^{-0.2863} \times VI\left(\frac{T_{on}}{T_{on}+T_{off}}\right)$$

$$= \frac{0.0523 \times V \times I^{1.7615} \times {T_{on}}^{0.7137}}{T_{on} + T_{off}}$$

But, $E_{MRR} = \rho V_W \left[C_p(T_v - T_o) + L_m + L_v\right]$

$$\frac{0.0523 \times V \times I^{1.7615} \times {T_{on}}^{0.7137}}{T_{on} + T_{off}} = \rho V_W \left[C_p(T_v - T_o) + L_m + L_v\right] \tag{7}$$

By putting the value of material properties of the workpiece in Equation (7) from Table 3,

$$V_W = \frac{12.7 \times 10^{-4} \times V \times I^{1.7615} \times {T_{on}}^{0.7137}}{T_{on} + T_{off}} mm^3/sec$$

$MRR = \frac{V_W}{60}$

$$MRR = \frac{0.0762 \times V \times I^{1.7615} \times {T_{on}}^{0.7137}}{T_{on} + T_{off}} mm^3/min \tag{8}$$

### 3.2. Tool wear rate

For the development of a model for TWR, the same procedure is used as discussed in the section of material removal rate. The regression equation for fraction of energy (%) responsible for tool wear obtained using MINITAB 16 is

$$F_{TWR} = 6.4412 \times I^{2.8593} \times {T_{on}}^{-2.2193} \tag{9}$$

$$TWR = \frac{0.0722 \times V \times I^{3.8593} \times {T_{on}}^{-1.2193}}{T_{on} + T_{off}} mm^3/\min \tag{10}$$

## 4. Results and discussion

Table 4 shows the experimental results of the material removal rate (MRR) and tool wear rate (TWR) at different levels of process parameters. 3D surface plots showing relations among discharge current, pulse on time, pulse off time, MRR, and TWR are plotted using statistical software MINITAB 16. The combined effect of all process parameters on MRR and TWR are shown in Figure 4 to 9. Based on the basic theory of material removal in EDM, the mathematical models for MRR and TWR have been developed in section 3.

Figure 4 shows that MRR increases with an increase in discharge current at the same pulse on time. This happens because an increase in discharge current produces a strong spark, which results in higher temperature and so melting of more material and erosion from the workpiece takes place. As per Figure 5, the interaction of MRR with discharge current and pulse off time follows the same pattern of behavior as of MRR with discharge current and pulse on time. To achieve maximum MRR, values of pulse on time and pulse off time should be kept at a lower level as shown in Figure 6. The tool wear rate decreases with an increase in pulse on time as shown in Figure 7. At a higher pulse on time, more heat energy is released between workpiece and tool which breaks down the dielectric fluid and releases carbon particles. These particles form a protective layer on the tool surface which reduces TWR. Figure 8 shows a 3D surface plot of TWR vs. pulse off time and discharge current. At the same current level, TWR decreases with an increase in pulse off time. This is expected because high pulse off time reduces discharge energy results in lower melting of material and reduction in tool wear. The combined effect of the pulse on time and pulse off time on TWR is shown in Figure 9. To achieve minimum TWR, pulse on time should be kept at a higher level and pulse off time should be kept at a lower level.

**Table 4.** Experimental result for MRR and TWR.

| Exp. No. | Impression Dia. D (mm) | Impression Depth H (mm) | MRR ($mm^3$/ min) | Initial Weight W1 (gm) | Final Weight W2 (gm) | TWR ($mm^3$/ min) |
|---|---|---|---|---|---|---|
| 1 | 12.608 | 1.216 | 10.12 | 21.9927 | 21.9920 | 0.0052 |
| 2 | 12.139 | 3.108 | 23.97 | 23.3707 | 23.2614 | 0.8130 |
| 3 | 12.543 | 0.507 | 4.17 | 25.1495 | 25.1494 | 0.0010 |
| 4 | 12.375 | 1.347 | 10.80 | 24.3242 | 24.3234 | 0.0057 |
| 5 | 12.342 | 0.620 | 4.94 | 22.8507 | 22.8505 | 0.0012 |
| 6 | 12.429 | 0.732 | 5.92 | 22.4281 | 22.4267 | 0.0104 |
| 7 | 12.365 | 1.443 | 11.55 | 22.8274 | 22.8215 | 0.0441 |
| 8 | 12.327 | 1.753 | 13.94 | 23.1767 | 23.1508 | 0.1924 |
| 9 | 12.621 | 0.572 | 4.77 | 23.2187 | 23.2151 | 0.0268 |
| 10 | 12.687 | 4.064 | 34.23 | 22.7660 | 22.5967 | 1.2597 |
| 11 | 12.224 | 1.561 | 12.21 | 24.6431 | 24.6363 | 0.0504 |
| 12 | 12.453 | 2.872 | 23.31 | 23.8024 | 23.7964 | 0.0446 |
| 13 | 12.250 | 0.676 | 5.31 | 21.8953 | 21.8908 | 0.0339 |
| 14 | 12.522 | 0.800 | 6.56 | 24.6102 | 24.6053 | 0.0364 |
| 15 | 12.303 | 3.411 | 27.02 | 24.0009 | 23.9618 | 0.2909 |
| 16 | 12.140 | 1.605 | 12.38 | 23.6588 | 23.6387 | 0.1498 |
| 17 | 12.179 | 0.582 | 4.52 | 22.3103 | 22.3093 | 0.0073 |
| 18 | 12.389 | 3.347 | 26.88 | 23.7383 | 23.5792 | 1.1835 |
| 19 | 12.503 | 1.334 | 10.91 | 22.7701 | 22.7692 | 0.0065 |

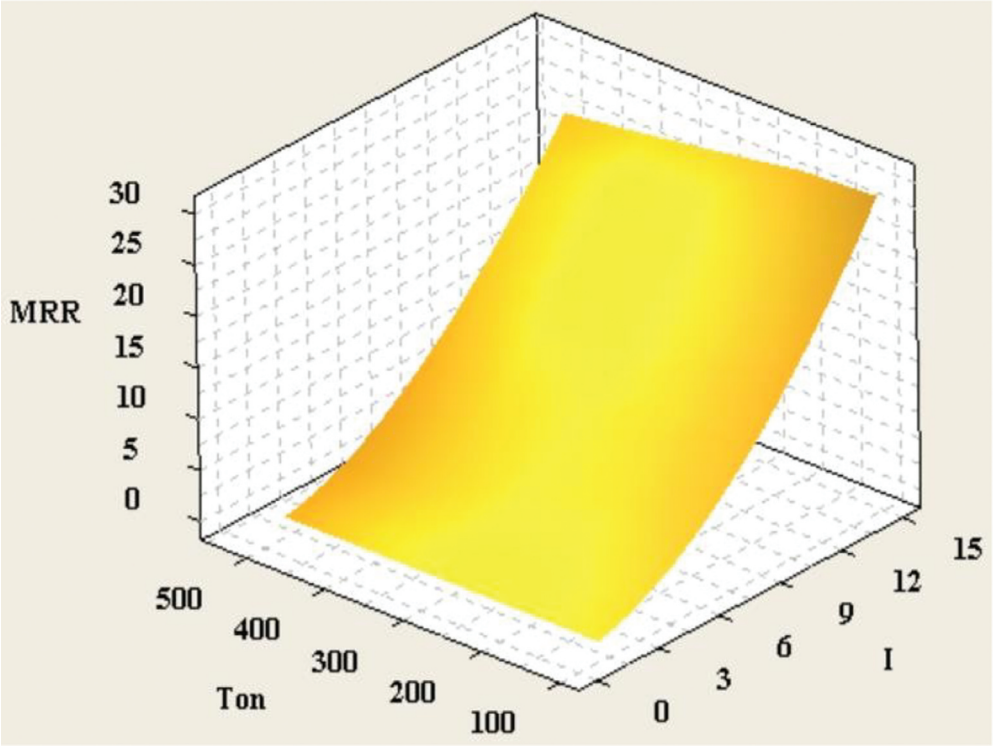


Figure 4. Surface plot of MRR vs. pulse on time and discharge current.

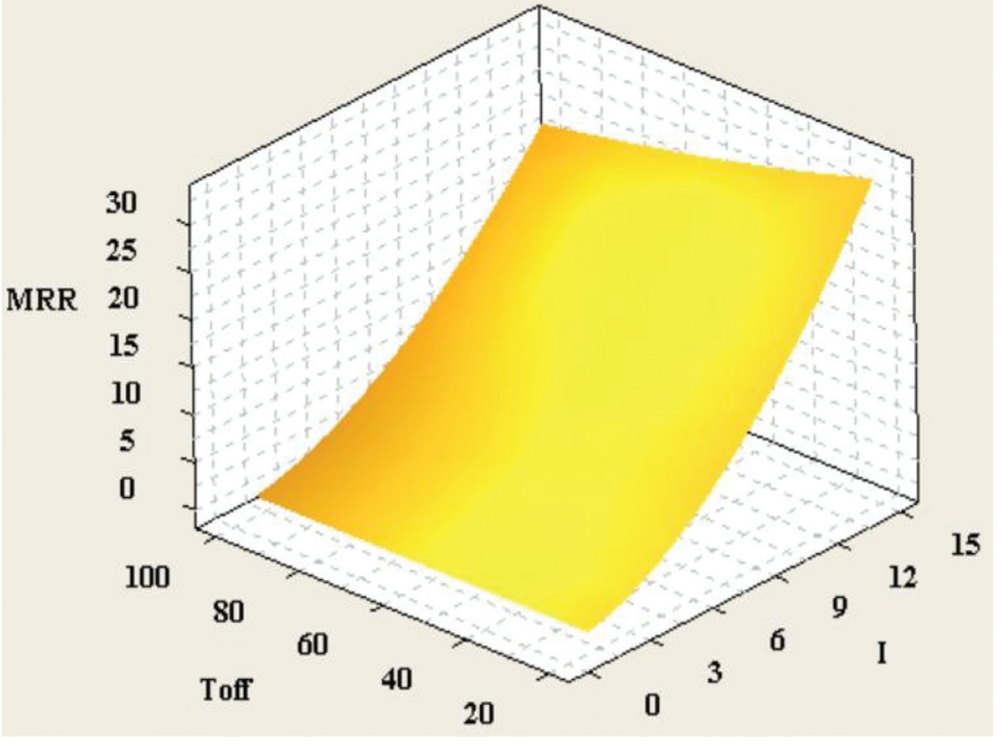


Figure 5. Surface plot of MRR vs. pulse off time and discharge current

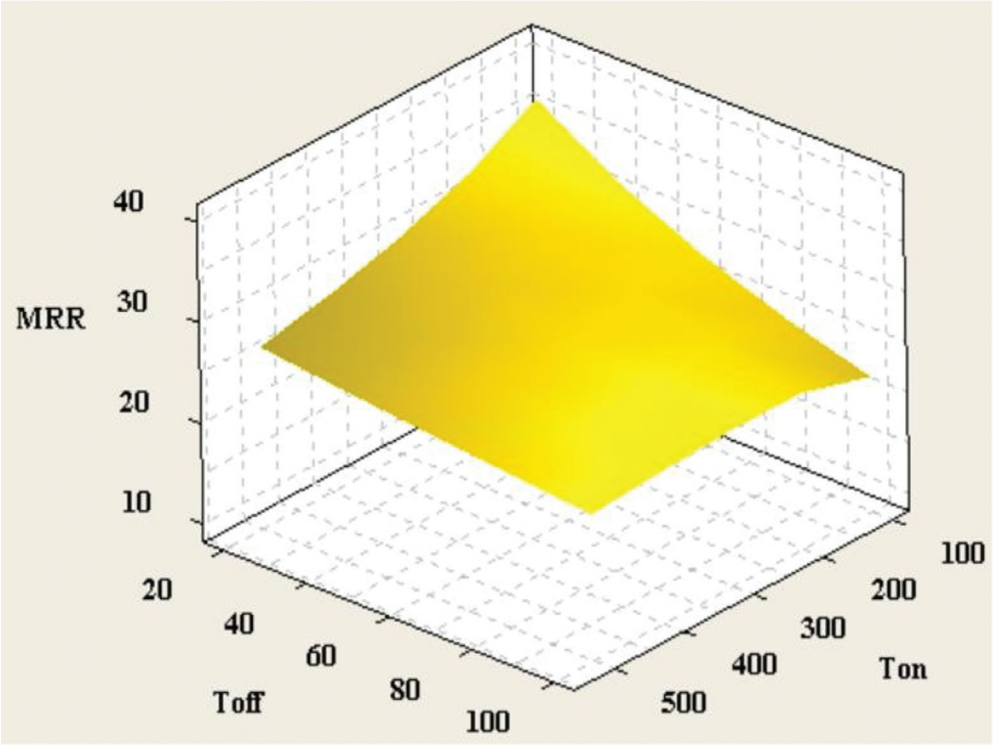


Figure 6. Surface plot of MRR vs. pulse off time and pulse on time.

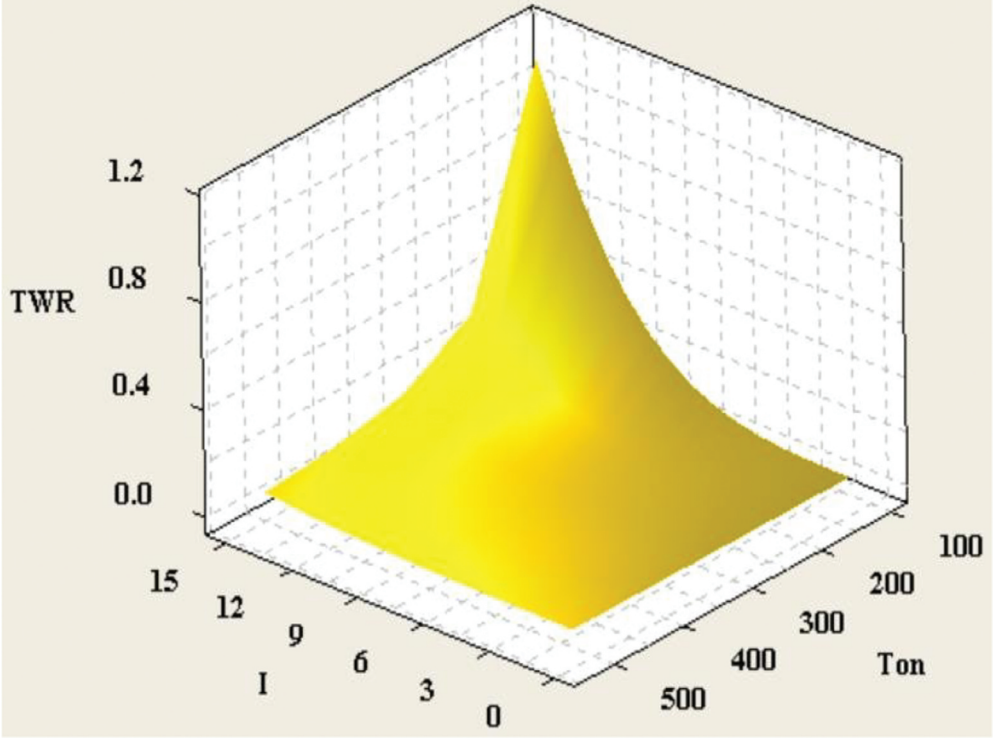


Figure 7. Surface plot of TWR vs. discharge current and pulse on time.

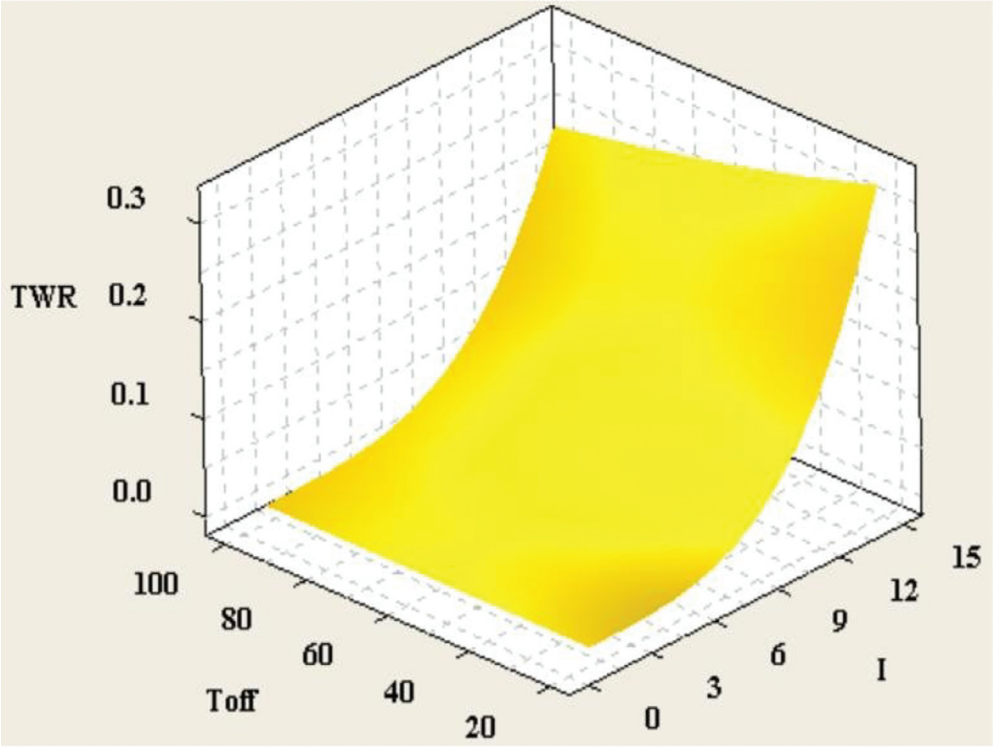


Figure 8. Surface plot of TWR vs. pulse off time and discharge current.

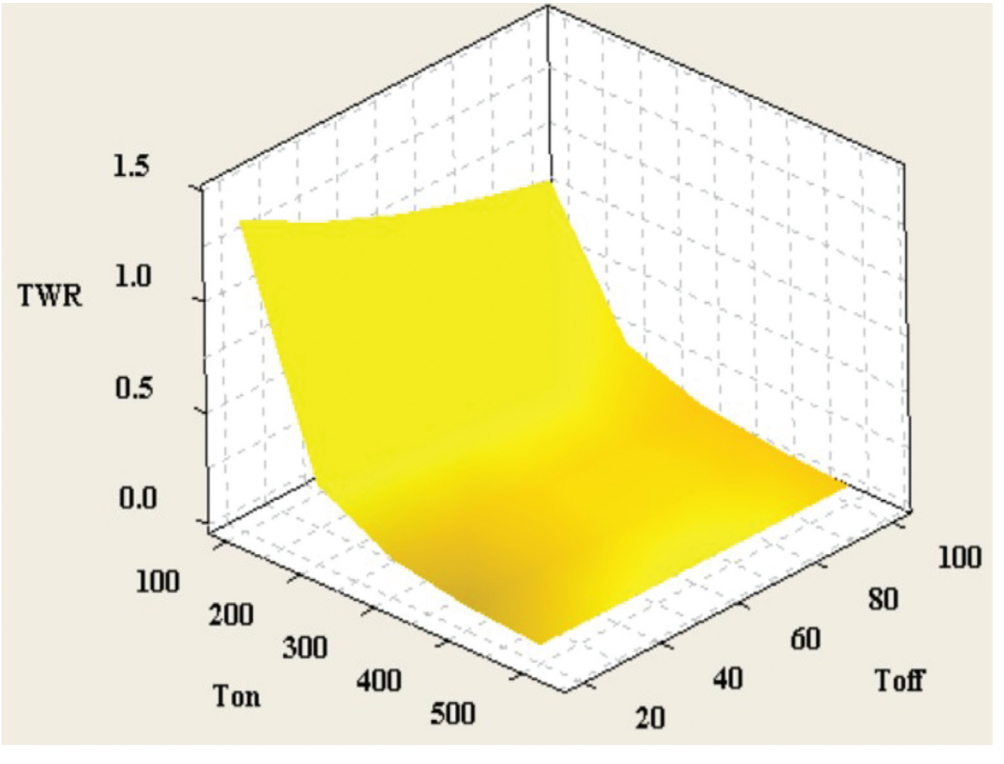


Figure 9. Surface plot of TWR vs. pulse on time and pulse off time.

**Table 5.** Comparison of results for MRR.

| Exp. No. | I (A) | Ton (μs) | Toff (μs) | MRR ($mm^3$/min) | | |
|---|---|---|---|---|---|---|
| | | | | Experiment | Predicted | % Error |
| 1 | 3 | 50 | 10 | 2.36 | 2.58 | 9.32 |
| 2 | 3 | 200 | 50 | 1.53 | 1.67 | 9.15 |
| 3 | 3 | 1000 | 200 | 1.02 | 1.10 | 7.84 |
| 4 | 9 | 50 | 50 | 11.35 | 10.73 | 5.46 |
| 5 | 9 | 200 | 200 | 7.31 | 7.22 | 1.23 |
| 6 | 9 | 1000 | 10 | 8.33 | 9.01 | 8.16 |
| 7 | 21 | 50 | 200 | 17.84 | 19.10 | 7.06 |
| 8 | 21 | 200 | 10 | 55.99 | 61.14 | 9.19 |
| 9 | 21 | 1000 | 50 | 35.89 | 38.57 | 7.46 |

**Table 6.** Comparison of results for TWR.

| Exp. No. | I (A) | Ton (μs) | Toff (μs) | TWR ($mm^3$/min) | | |
|---|---|---|---|---|---|---|
| | | | | Experiment | Predicted | % Error |
| 1 | 3 | 50 | 10 | 0.0124 | 0.0127 | 2.41 |
| 2 | 3 | 200 | 50 | 0.0006 | 0.0006 | 0.00 |
| 3 | 3 | 1000 | 200 | 0.0000 | 0.0000 | 0.00 |
| 4 | 9 | 50 | 50 | 0.5708 | 0.5308 | 7.00 |
| 5 | 9 | 200 | 200 | 0.0264 | 0.0245 | 7.19 |
| 6 | 9 | 1000 | 10 | 0.0015 | 0.0014 | 6.66 |
| 7 | 21 | 50 | 200 | 5.3593 | 5.5867 | 4.24 |
| 8 | 21 | 200 | 10 | 1.1390 | 1.2268 | 7.70 |
| 9 | 21 | 1000 | 50 | 0.0354 | 0.0345 | 2.54 |

### 4.1. Validation of models

To investigate the validity of the mathematical models for MRR & TWR, new experiments were designed based on Taguchi's L9 orthogonal array using different values of process parameters as shown in Tables 5 & 6 respectively. These table also show the results of validation experiments as well as prediction values of MRR and TWR from mathematical models.

Figures 10 and 11 show a comparison of validation experiments and predicted values for MRR & TWR in the form of scatter plots respectively. In both the plots, the points are

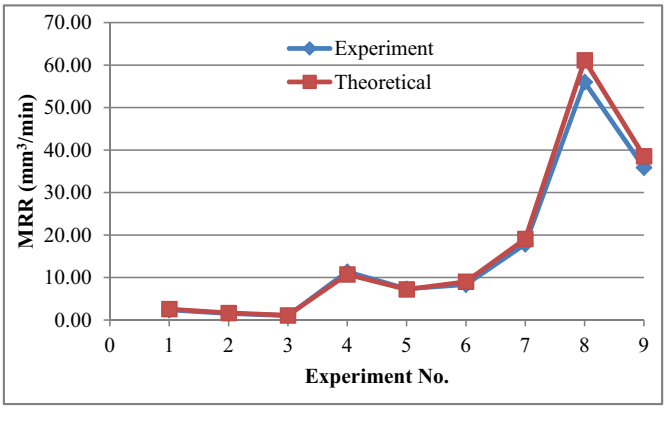


**Figure 10.** Comparison of experimental and theoretical results for MRR.

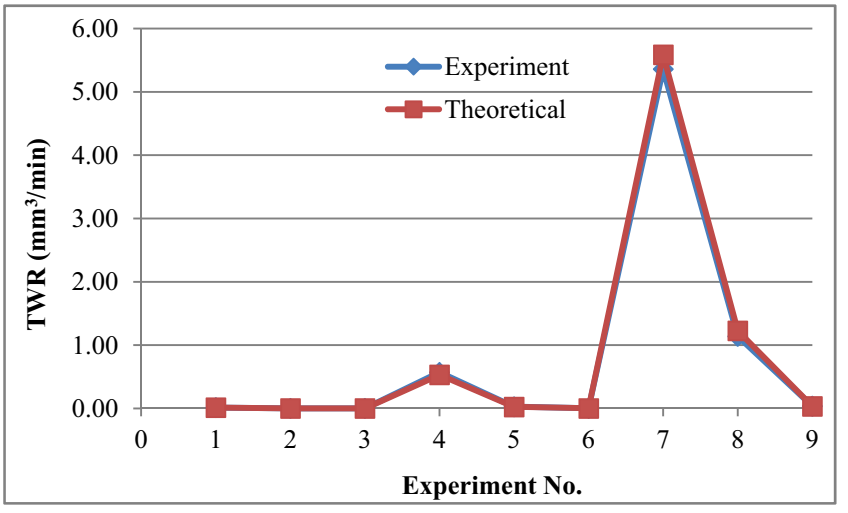


Figure 11. Comparison of experimental and theoretical results for TWR.

Table 7. Comparison of MRR ratio.

| Model No. | Model | Range of MRR Ratio |
|---|---|---|
| 1 | Snoeys's model [39] | 3.9–203.2 |
| 2 | Van Dijck's model [39] | 26.8–1399 |
| 3 | Beck's model [39] | 4.9–197.7 |
| 4 | Jilani's model [39] | 2–45.9 |
| 5 | DiBitonto's model [39] | 1.2–46.1 |
| 6 | Our model | 0.9–1 |

overlapping for almost all readings and hence, there is no significant difference between experimental and theoretical results. This means the models of MRR and TWR are also valid for the values of process parameters beyond the selected values for the development of models.

The MRR ratios (predicted result to experimental data) from electro-thermal based models of different researchers are compared as shown in Table 7 and it is found that prediction accuracy of our model is much better than other models., The researchers have considered the fraction of energy transfer to the workpiece as 50% of discharge energy in models 1–4, 18% in model 5 and variable in model 6. This proves that the fraction of energy transfer plays an important role in predicting material removal from workpiece and tool.

## 5. Conclusion

Different techniques have been used by researchers for modeling of performance measures of EDM like MRR, TWR, etc. Each technique has certain limitations due to some assumptions for the simplification of models. In this article, a new technique for the development of mathematical models for MRR and TWR is described considering thermo-mechanical theory for material removal in EDM. The energy responsible for MRR and TWR was calculated based on melting and evaporation of material as well as

regression equations for the same were developed. These equations were utilized for the development of mathematical models of MRR and TWR. The full factorial design was used for the design of experiments and according to that, a total of 27 experiments were conducted. To check the validity of models for a different set of process parameters, nine experiments were conducted based on Taguchi's L9 orthogonal array design and their results were compared with the predicted MRR and TWR. It was found that the results predicted by the proposed models of MRR and TWR have a close agreement with the experimental results and have good prediction accuracy than other models due to consideration of variable fraction of energy transfer to the workpiece and tool based on process parameters. Hence, this approach can be used to predict MRR and TWR at any set of process parameters for different combinations of workpiece and tool.

## Disclosure statement

No potential conflict of interest was reported by the authors.

## ORCID

C. R. Sanghani http://orcid.org/0000-0001-8369-8827

## References

[1] Escobar AM, De Lange DF, Medellin Castillo HI. Comparative analysis and evaluation of thermal models of electro discharge machining. Int J Adv Manuf Technol. 2017;89 (1–4):743–754.
[2] DiBitonto DD, Eubank PT, Patel MR, et al. Theoretical models of the electrical discharge machining process-I: a simple cathode erosion model. J Appl Phys. 1989;66:4095–4103.
[3] Patel MR, Barrufet MA, Eubank PT, et al. Theoretical models of the electrical discharge machining process-II: the anode erosion model. J Appl Phys. 1989;66:4104–4111.
[4] Eubank PT, Patel MR, Barrufet MA, et al. Theoretical models of the electrical discharge machining process-III: the variable mass, cylindrical plasma model. J Appl Phys. 1993;73:7900–7909.
[5] Gulbinowicz Z, Goroch O, Skoczylas P. Mathematical modeling of material erosion during the electrical discharge. Adv Sci Technol Res J. 2020;14(2):27–33.
[6] Singh A, Ghosh A. A thermo-electric model of material removal during electric discharge machining. Int J Mach Tools Manuf. 1999;39:669–682.
[7] Yeo SH, Kurnia W, Tan PC. Electro-thermal modelling of anode and cathode in micro-EDM. J Phys D: Appl Phys. 2007;40:2513–2521.
[8] Salonitis K, Stournaras A, Stavropoulos P, et al. Thermal modeling of the material removal rate and surface roughness for die-sinking EDM. Int J Adv Manuf Technol. 2009;40:316–323.
[9] Wang PJ, Tsai KM. Semi-empirical model on work removal and tool wear in electrical discharge machining. J Mater Process Technol. 2001;114(1):1–17.
[10] Jeswani ML. Dimensional analysis of tool wear in electrical discharge machining. Wear. 1979;55:153–161.
[11] Tsai KM, Wang PJ. Semi-empirical model of surface finish on electrical discharge machining. Int J Mach Tools Manuf. 2001;41:1455–1477.
[12] Dave HK, Desai KP, Raval HK. Development of semi empirical model for predicting material removal rate during orbital electro discharge machining of Inconel 718. Int J Mach Machinability Mater. 2013;13(2/3):215–230.

[13] Kumar S, Singh R, Batish A. et al. Modeling the tool wear rate in powder mixed electro-discharge machining of titanium alloys using dimensional analysis of cryogenically treated electrodes and workpiece. Proc. Inst Mech Eng Part E. J Process Mech Eng. 2015;231 (2):271–282.
[14] Yahya A, Manning CD. Determination of material removal rate of an electro-discharge machine using dimensional analysis. J Phys D: Appl Phys. 2004;37:1467–1471.
[15] Bhaumik M, Maity K, Mohapatra KD. Determination of material removal rate and radial overcut in electro discharge machining of AISI 304 using dimensional analysis. Appl Mech Mater. 2016;852:160–165.
[16] Schulze H, Herms R, Juhr H, et al. Comparison of measured and simulated crater morphology for EDM. J Mater Process Technol. 2004;149:316–322.
[17] Lasagni A, Soldera F, Mucklich F. FEM simulation of local heating and melting during electrical discharge plasma impact. Modelling Simul Mater Sci Eng. 2004;12:835–844.
[18] Joshi SN, Pande SS. Thermo-physical modeling of die-sinking EDM process. J Manuf Processes. 2010;12(1):45–56.
[19] Ming W, Zhang G, Li H, et al. A hybrid process model for EDM based on finite-element method and Gaussian process regression. Int J Adv Manuf Technol. 2014;74:1197–1211.
[20] Tang J, Yang X. A thermo-hydraulic modeling for the formation process of the discharge crater in EDM. Procedia CIRP. 2016;42:685–690.
[21] Zhang F, Gu L, Hu J, et al. A new thermal model considering TIE of the expanding spark for anode erosion process of EDM in water. Int J Adv Manuf Technol. 2016;82(1):573–582.
[22] Yildiz Y. Prediction of white layer thickness and material removal rate in electrical discharge machining by thermal analyses. J Manuf Processes. 2016;23:47–53.
[23] Assarzadeh S, Ghoreishi M. Prediction of root mean square surface roughness in low discharge energy die-sinking EDM process considering the effects of successive discharges and plasma flushing efficiency. J Manuf Processes. 2017;30:502–515.
[24] Huang H, Zhang Z, Ming W, et al. A novel numerical predicting method of electric discharge machining process based on specific discharge energy. Int J Adv Manuf Technol. 2017;88(1–4):409–424.
[25] Wu H, Ma J, Meng Q, et al. Numerical modeling of electrical discharge machining of Ti-6Al-4V. Procedia Manuf. 2018;26:359–371.
[26] Klocke F, Mohammadnejad M, Zeis M, et al. Investigation on the variability of existing models for simulation of local temperature field during a single discharge for electrical discharge machining (EDM). Procedia CIRP. 2018;68:260–265.
[27] Jatti VS, Bagane S. Thermo-electric modelling, simulation and experimental validation of powder mixed electric discharge machining (PMEDM) of BeCu alloys. Alexandria Eng J. 2018;57:643–653.
[28] Jithin S, Raut A, Bhandarkar UV, et al. FE modeling for single spark in EDM considering plasma flushing efficiency. Procedia Manuf. 2018;26:617–628.
[29] Bergs T, Schneider S, Harst S, et al. Numerical simulation and validation of material loadings during electrical discharge machining. Procedia CIRP. 2019;82:14–19.
[30] Liu C, Duong N, Jahan MP, et al. Experimental investigation and numerical simulation of micro-EDM of bulk metallic glass with focus on crater sizes. Procedia Manuf. 2019;34:275–286.
[31] Puertas I, Luis CJ, Alvarez L. Analysis of the influence of EDM parameters on surface quality, MRR and EW of WC–Co. J Mater Process Technol. 2004;153–154:1026–1032.
[32] Chattopadhyay KD, Verma S, Satsangi PS, et al. Development of empirical model for different process parameters during rotary electrical discharge machining of copper–steel (EN-8) system. J Mater Process Technol. 2009;209:1454–1465.
[33] Izwan NSL, Feng Z, Patel JB, et al. Prediction of material removal rate in die-sinking electrical discharge machining. Procedia Manuf. 2016;5:658–668.
[34] Puthumana G. Micro-EDM process modeling and machining approaches for minimum tool electrode wear for fabrication of biocompatible micro-components. J Machine Eng. 2017;17 (3):97–111.

[35] Hosni NJ, Lajis MA, Idris MR. Modelling and optimization of chromium powder mixed edm parameter effect over the surface characteristics by response surface methodology approach. Int J Eng Mater Manuf. 2018;3(2):78–86.
[36] Perveen A, Jahan M. Modeling and optimization of crater size generated during micro-EDM of Ti alloy using Response surface method. Mater Today Proc. 2018;5 (9):18307–18314.
[37] Shen Y, Liu Y, Zhang Y, et al. Determining the energy distribution during electric discharge machining of Ti–6Al–4V. Int J Adv Manuf Technol. 2014;70:11–17.
[38] Singh H. Experimental study of distribution of energy during EDM process for utilization in thermal models. Int J Heat Mass Transf. 2012;55(19):5053–5064.
[39] Yeo SH, Kurnia W, Tan PC. Critical assessment and numerical comparison of electro-thermal models in EDM. J Mater Process Technol. 2008;(2008(203):241–251.